DOI: 10.61782/fa.2025.0691

FORUM ACUSTICUM EURONOISE 2025

PREDICTING THE EFFECTS OF GROUND IMPEDANCE IN LONG-RANGE LOW-FREQUENCY PROPAGATION WITH THE SEMI-ANALYTIC FINITE-ELEMENT (SAFE) METHOD.

Rafael Castro Mota[1,2*] **Paul Williams**[3] **Ray Kirby**[4] **Stefan Jacob**[1,2]

[1] Physikalisch-Technische Bundesanstalt, Braunschweig, Germany
[2] Technische Universität Braunschweig, Braunschweig, Germany
[3] University of Technology Sydney, Sydney, Australia
[4] RMIT University, Melbourne, Australia

ABSTRACT

The outdoor propagation of infrasound can be impacted by atmospheric conditions, such as temperature inversions and winds, that channel sound into acoustic waveguides allowing for efficient long-range propagation. For near ground acoustic waveguides, ground impedance can also play an important role. In this study, the Semi-Analytic Finite Element (SAFE) method is used to predict the acoustic field generated by a point source emitting into a stratified, range independent atmosphere with a logarithmic wind profile. We study the influence of ground impedance by setting two cases with different ground boundary conditions: a fully reflective ground condition, mimicking sea propagation; and an impedance ground boundary condition, mimicking a sandy landscape. We found a significant contrast in the two test cases for the near-ground acoustic waveguides, especially for a particular near-ground acoustic mode. Thus, ground impedance should be included in predictions

Keywords: *low-frequency sound, outdoor propagation, normal-mode methods*

**Corresponding author*: rafael.castro-mota@ptb.de

1. INTRODUCTION

The outdoor propagation of infrasound can be impacted by atmospheric conditions, such as temperature inversions and winds. By refracting sound downwards, acoustic energy gets channeled into acoustic waveguides, reducing geometric spreading. Lower frequencies, notably infrasound, which experience decreased atmospheric damping, can travel efficiently inside these ducts, leading to increased sound pressure levels down-range of an emitter. For highly refracting conditions, near-ground waveguides can be dominant features in the acoustic field and, due to their interaction with the ground, be influenced by the acoustic behavior of this surface.

Large energy converters such as wind turbines and biogas power plants are possible emitters in the lower frequency spectrum and, when installed next to populated areas, raise concerns regarding exposure levels and annoyance. Accurate prediction of the noise levels at these locations is important and depends on a good understanding of the influence of the ground surface on the acoustic field.
Numerical predictions for the outdoor propagation of sound tend to either be heavy, due to large domain size, or rely on approximations, to reduce computational costs. The semi analytical finite-element (SAFE) method has been introduced by Kirby as an alternative to PEs to model outdoor sound propagation for range-independent domains [1], [2]. The procedure translates the acoustic field into a set of vertical atmospheric acoustic modes, propagating in the down-range direction. The method was originally introduced by Waxler [3] with numerical solutions for modes based on

an approximate wave equation. Using the SAFE method enables the solution of the exact governing equations with arbitrary atmospheric profiles while being able to accommodate a range-independent Ingard-Myers impedance boundary condition at the ground level [2]. The SAFE method has been tested against analytic solutions [1] and validated against test cases computed with the direct numerical computations of the Linearized Euler Equations [4]. It has also been shown to be particularly efficient for highly refracting atmospheres, requiring a limited number of modes for accurate near-ground far-field predictions [5].

In this study, the Semi-Analytic Finite-Element (SAFE) method is used to predict the acoustic field generated by a point source emitting into a stratified, range-independent atmosphere with a logarithmic wind profile. We study the influence of ground impedance by setting two cases with different ground boundary conditions: a fully reflective ground condition, mimicking sea propagation; and an impedance ground boundary condition, mimicking a sandy landscape. In the downwind direction, we found a significant contrast for the near-ground acoustic waveguides while the acoustic field at higher altitudes is significantly less affected. We conclude that ground impedance should be included in near-ground predictions as it plays an important part in both amplitude and distribution of sound pressure levels.

2. SAFE METHOD

The SAFE method is derived and discussed with more extent in [1], [2]. A short description is given here.

The method starts with an accurate pressure equation for acoustic waves propagating in stratified, range-independent atmospheres for frequencies above the Brunt-Väisälä limit, nominally 0.05 Hz (from [6], Eq. 2.58).

$$\left[\frac{1}{c^2}D_t^3 - D_t\left(\frac{\partial^2}{\partial x^2}+\frac{\partial^2}{\partial z^2}+2\tilde{g}\,\frac{\partial}{\partial z}+\tilde{g}^2-\frac{2\tilde{g}}{c}\frac{\partial c}{\partial z}\right)+ 2\frac{\partial u_0}{\partial z}\frac{\partial}{\partial x}\left(\tilde{g}+\frac{\partial}{\partial z}\right)+\left(2\tilde{g}+\frac{1}{\rho}\frac{\partial \rho_0}{\partial z}\right)D_t\left(\tilde{g}+\frac{\partial}{\partial z}\right)\right]p' = \rho D_t^2 Q, \quad (1)$$

where p' is the acoustic pressure, ρ' is the acoustic density, u_0 is the background velocity in the range direction (x), $\tilde{g}$ is the acceleration of gravity divided by the speed of sound squared ($\tilde{g}=\frac{g}{c^2}$), Q is a mass source, $D_t=(\frac{\partial}{\partial t}+u_0\frac{\partial}{\partial t})$, x denotes the range coordinate, z the height coordinate and t denotes time. This two-dimensional equation results from assuming a stratified atmosphere in a linearized two-dimensional Euler equation

$$\begin{cases}\frac{d\rho'}{dt}+(V'\cdot\nabla)\rho_0+\rho_0\nabla\cdot V'+\rho'\nabla\cdot V_0=\rho_0 Q\\ \frac{dV'}{dt}+(V'\cdot\nabla)V_0+\frac{1}{\rho_0}\nabla p'-\frac{\rho'\nabla p_0}{\rho}=F\\ \frac{ds'}{dt}+(V'\cdot\nabla)s_0=0\end{cases}, (2)$$

with F being a force source, (ρ_0,p_0,V_0) being quantities related to the background field, namely, density, pressure and velocity, and (ρ',p',V') the same quantities for the acoustic field.

The pressure field may be expressed as a sum of range propagating vertical modes, following the Ansatz

$$p'(x,z,t)=\sum_{n=1}^{\infty}A_n p_n(z)e^{iwt-ik_0\gamma_n x}, \qquad (3)$$

where A is the complex mode amplitude, p_n are the mode shapes, k_0 is the reference wave number and γ_n are the eigenvalues associated with the mode shapes. Equation 1 then turns into an eigenvalue problem in the height coordinate

$$+k^2[1-\gamma M]^3p' + [1+\gamma M]\left\{\left(\tilde{g}^2-\frac{2\tilde{g}}{c}\frac{\partial c}{\partial z}\right)+2\tilde{g}\frac{\partial}{\partial z}+\frac{\partial^2}{\partial z^2}-k_0^2\gamma^2\right\}p' + 2\gamma\frac{\partial M}{\partial z}\left(\tilde{g}+\frac{\partial}{\partial z}\right)p' - \left[2\tilde{g}+\frac{1}{\rho}\frac{\rho}{\partial z}\right][1-\gamma M]\left(\tilde{g}+\frac{\partial}{\partial z}\right)p' = 0, \qquad (4)$$

with M being the Mach number [4,5].
Equation 4 can be solved using the finite-element method and an eigen solver. The ground impedance ($\tilde{Z}$) is set on the finite-element approximation by following the steps in [2] and using the Ingard-Myers boundary condition expressed as a function of purely acoustic pressure.

$$\frac{\partial p'(0)}{\partial z}=\left[\frac{ik_0}{\tilde{Z}}(1-\gamma M_0)^2+\tilde{g}_0\right]p'(0), \qquad (4)$$

For the test cases shown here, we use an in-house FE solver, based on quadratic elements and the *eig* function from the scientific Python package *numpy*. More details about the method and the weak formulation of the eigenvalue problem are available in Refs [1], [2].

The modes' amplitudes are computed by employing a vertical mode matching scheme that was derived to mimic a harmonic point source. Details about the mode matching can again be found in Refs [1], [2].

3. RESULTS

We computed two cases with the same atmospheric conditions: $u_0 = 2.33 \cdot \ln(1 + 2.3z), v_0 = 0,$ $t_0 = 293.15\,K,$ $\rho_0 = 1.23\,Kg/m^3,$ and $p_0 = 1\,atm;$ and different ground impedances, namely: a fully reflective ground surface ($\tilde{Z} = \infty$), mimicking sea propagation; and an impedance ground boundary condition ($\tilde{Z} = 38.79 - 38.41i$), mimicking a sandy landscape. For both test cases, the acoustic field was excited via a 10 Hz point source placed at the origin of the range coordinate and at height of 100m.

Figures 1.a) and 1.b) show a normalized pressure contour plot for both scenarios. The acoustic pressure has been normalized with the maximum recorded acoustic pressure for each. Downwind from the source, the plots show significant differences close to the ground, whereby the lower-altitude acoustic waveguide visible in Figure 1.a) is not evident in Figure 1.b). Below 250m, the remaining acoustic features related to atmospheric ducting are visible in both plots, having more contrast in Figure 1.a). For higher altitudes, both plots are qualitatively very similar. In the upwind direction, the acoustic field seems to not have been significantly affected by the difference in ground impedance.

The acoustic transmission, at the heights of, respectively, 1.8m and 500m, is plotted in Figures 1.c) and 1.d), along a range extending from -5km to 20km. At each height, the results for the two ground impedances are presented with the maximum recorded acoustic pressure being used as a reference. In Figure 1.c), the transmission recorded at 1.8m is evidently affected by the addiction of a ground-impedance, with a clear alteration in the downwind near-ground ducted pattern, being starker for the fully reflective ground surface. The acoustic field appears as more dampened for the sandy landscape scenario. Figure 1.d) indicates a quantitively similar transmission between both scenarios at an altitude of 500 m. At both heights, results in the upwind direction are similar.

Having noted a more prevalent effect on the near-ground acoustic field of the ground impedance change, five modes have been selected. These are modes that are important to the far-field (low dampening) and concentrate at least 15 per cent of their energy (signal energy) below 250 m. Figures 1.c) and 1.d) show that while these modes are not sufficient for an accurate prediction, at 500m, they provide good results for the near-ground far field, where the field is more affected by the change in impedance.

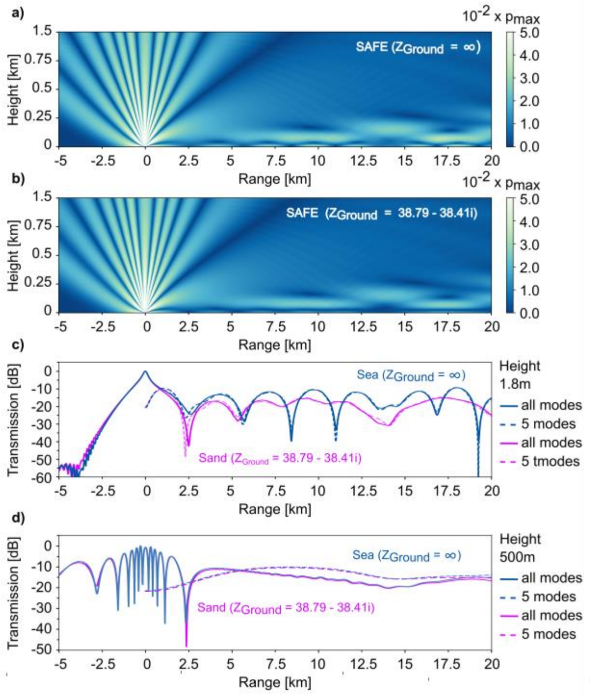

Figure 1. Normalized pressure contours of a point source radiating sound at 10 Hz in a atmosphere with a logarithmic wind profile and constant temperature and pressure for a) a fully reflective sea surface and b) a sandy landscape ($\tilde{Z} = 38.79 - 38.41i$). Transmission Loss along a horizontal line at a height of c) 1.8 m, d) 500m.

With the near-ground far-field prediction reduced to five propagating modes, a mode decay plot for each of the two cases is shown, respectively, in Figures 2.a) and 2.b). The modes have been paired up by how close their real parts are and given a numbering. Comparing the two figures, mode 5 seems to have been, by far, the most affected by the change in ground impedance. By looking at Figure 1.c), where the real and imaginary parts have been plotted for each case, one can check that the energy of the mode is highly concentrated near the ground and that the overall modal shape has not been severely altered. The respective eigenvalues of 0.972860-0.000996j (sand) and 0.971968-

1.205441e-06j (sea) also show that the phase-speed of the mode (real part), has almost been retained, with the attenuation of the mode (imaginary part) having been significantly increased.

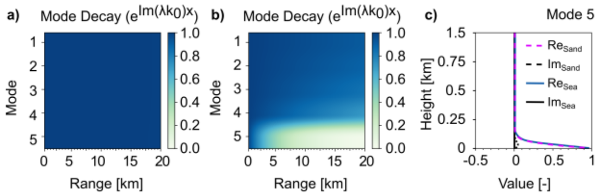

Figure 2. Modal decay plot for a) sea and b) sandy surface and a logarithmic wind profile. c) The real and imaginary parts for the 5th mode in the sea and sand surface test cases.

4. FINAL COMMENTS AND CONCLUSIONS

The purpose of this paper was to dwell into the influence of ground acoustic impedance for acoustic propagation in a highly refracting atmosphere. We did this by comparing the results of the SAFE method in two different test scenarios, each with the same atmosphere with a logarithmic wind profile and a different ground impedance: the 1st variation mimicking propagation along a fully reflective sea surface and the 2nd along a sandy landscape. Downwind from the source, the computations showed a significant change in the near-ground acoustic field, indicating a strong dampening of acoustic modes closer to the ground. Apart from the near-ground field, the acoustic field below 250m seems less sensitive to the change, with the same patterns in the contour plots being visible. Upwind from the source, we speculate that the upward refracting effect of the atmosphere contributed to a clear insensitivity to the change in ground impedance. The results for the higher altitudes in both directions presented themselves as almost unchanged. By reducing the modal base down to five modes, we deciphered that one mode was particularly affected by the change in ground impedance. We conclude that, in the context of highly refracting atmospheres, ground impedance plays a bigger role in near-ground predictions and that a limited number of modes, with most of its energy near the ground, experience noticeable changes. This result appears to indicate that there might be a reduction in complexity for predicting acoustic in highly-refracting atmospheres with ground impedances jumps by focusing the analysis on the more affected modes.

5. ACKNOWLEDGMENTS

This research is funded by the Deutsche Forschungsgemeinschaft (DFG, German Research Foundation) – JA 3325/2-1“

6. REFERENCES

[1] R. Kirby, “Atmospheric sound propagation in a stratified moving media: Application of the semi analytic finite element method,” *J. Acoust. Soc. Am.*, vol. 148, no. 6, pp. 3737–3750, Dec. 2020, doi: 10.1121/10.0002912.

[2] R. Kirby, “Atmospheric sound propagation in a moving fluid above an impedance plane: Application of the semi-analytic finite element method,” *J. Acoust. Soc. Am.*, vol. 149, no. 2, pp. 1285–1295, Feb. 2021, doi: 10.1121/10.0003567.

[3] R. Waxler, J. Assink, and D. Velea, “Modal expansions for infrasound propagation and their implications for ground-to-ground propagation,” *J. Acoust. Soc. Am.*, vol. 141, no. 2, pp. 1290–1307, Feb. 2017, doi: 10.1121/1.4976067.

[4] R. MOTA, R. KIRBY, P. WILLIAMS, and S. JACOB, “Efficient modeling of atmospheric infrasound propagation with the Semi-Analytical-Finite-Element (SAFE) method,” *INTER-NOISE NOISE-CON Congr. Conf. Proc.*, vol. 270, pp. 2711–2718, Oct. 2024, doi: 10.3397/IN_2024_3223.

[5] R. Castro Mota, R. Kirby, P. Williams, and S. Jacob, “Modelling Low-Frequency Sound Propagation in a Ducted Atmosphere Using a Semi-Analytic Finite-Element Method,” in *Proceedings of Acoustics 2024*, Gold Coast, Australia, Nov. 2024.

[6] V. Ostashev and D. Wilson, *Acoustics in Moving Inhomogeneous Media, Taylor & Francis (2015).*, 2nd ed. Taylor & Francis, 2015. [Online]. Available: https://doi.org/10.1201/b18922